Journal homepage: http://gwse.iheg.org.cn

Evaluation of the scaling and corrosion in Tai'an geothermal water, China

Man Li[1,2], Wei Zhang[1,2*], Yu-zhong Liao[1,2], Feng Liu[1,2], Long Li[1,2]

[1] *The Institute of Hydrogeology and Environmental Geology, Chinese Academy of Geological Sciences, Shijiazhuang* 050061, *China*.
[2] *Technology Innovation Center for Geothermal & Hot Dry Rock Exploration and Development, Ministry of Natural Resources, Shijiazhuang* 050061, *China*.

Abstract: Tai'an city, located in Shandong Province, China, is rich in geothermal resources, characterized by shallow burial, high water temperature, and abundant water supply, making them high value for exploitation. However, corrosion and scaling are main challenges that hinder the widespread application and effective utilization of geothermal energy. This study focuses on the typical geothermal fields in Tai'an, employing qualitative evaluations of the geochemical saturation index with temperature, combined with the corrosion coefficient, Ryznar index, boiler scale, and hard scale assessment, to predict corrosion and scaling trends in the geothermal water of the study area. The results show that the hydrochemical types of geothermal water in the study area are predominantly Na-Ca-SO_4 and Ca-Na-SO_4-HCO_3, with the water being weakly alkaline. Simulations of saturation index changes with temperature reveal that calcium carbonate scaling is dominant scaling type in the area, with no evidence of calcium sulfate scaling. In the Daiyue Qiaogou geothermal field, the water exhibited corrosive bubble water properties, moderate calcium carbonate scaling, and abundant boiler scaling. Feicheng Anjiazhuang geothermal field showed non-corrosive bubble water, moderate calcium carbonate scaling, and significant boiler scaling. The Daidao'an geothermal field presented corrosive semi-bubble water, moderate calcium carbonate scaling, and abundant boiler scaling. The findings provide a foundation for the efficient exploitation of geothermal resources in the region. Implementing anti-corrosion and scale prevention measures can significantly enhance the utilization of geothermal energy.

Keywords: Geothermal; Tai'an; Scaling; Corrosion; Central Shandong Uplift Area

Received: 08 May 2024/ Accepted: 30 Sep 2024/ Published online: 29 Nov 2024

Introduction

Corrosion and scaling are key challenges in the exploitation and utilization of geothermal resources (Zhu, 2006; Gallup, 2009; Pazheri et al. 2014). These issues arise from the complex interactions between chemical components and materials under varying conditions of temperature, flow rate, and pressure. Whether in geothermal power generation, heating, or other direct applications, corrosion frequently affects wellhead devices, pipes, and heat exchangers (Arteaga et al. 2013; Zarrouk et al. 2014; Liu, 2015). These challenges severely limit the widespread application and efficient utilization of geothermal energy (Stahl et al. 2000; Lv, 2020).

Understanding the chemical composition of geothermal water and predicting its corrosion and scaling tendencies are crucial for effectively managing geothermal water systems. While many studies have focused on scaling prediction, most emphasize carbonate and silicate scaling. Predictive indices, such as the Ryznar Index (RI) (Ryznar et al. 1944), Larson Index (LI) (Larson et al. 1967), Langelier Saturation Index (LSI) (Langelier, 2011), and Riddick Index (Riddick, 1944), are commonly used to evaluate scaling tendencies (Pátzay et al. 1998). Arnorsson et al. (1982) utilized the WATCH water chemistry program to predict scaling trends in Icelandic geothermal water. With advances in computational tools, an increasing number of scholars have used simulation software such as PHREEQC to calculate mineral saturation index, coupled with these above indices to predict scaling tendencies (Florent et al.

*Corresponding author: Wei Zhang, *E-mail address*: 18879003@qq.com

DOI: 10.26599/JGSE.2025.9280044

Li M, Zhang W, Liao YZ, et al. 2025. Evaluation of the scaling and corrosion in Tai'an geothermal water, China. Journal of Groundwater Science and Engineering, 13(2): 133-146.

2000; Appelo et al. 2005; Marimuthu et al. 2005; Delalande et al. 2011; Manan et al. 2023). In China, calcium carbonate scaling is predominant in geothermal systems. Researchers utilize complementary approaches combining the Ryznar and Larson indices for more accurate predictions (Zhu et al. 2004; Wei et al. 2012; Wang et al. 2015). Recent methodologies include hydrogeochemical simulations to predict corrosion and scaling tendencies (Liang et al. 2020; He et al. 2022; Pang et al. 2023). These methodologies encompass utilizing index calculation along with the WATCH simulation outcomes to ascertain scaling tendencies (Yu et al. 2007; Wei et al. 2012), integrating index calculations with mineral saturation indices to identify scaling types (Zhang et al. 2016; Song et al. 2020), and establishing quantitative models for calcium carbonate scaling in wellbores (Cen et al. 2022; Lin, 2022; Lei et al. 2023).

Shandong Province, hosts a significant distribution of geothermal resources, divided into three major geothermal anomaly zones: Eastern Shandong, South Central Shandong, and Southwestern Shangdong. Tai'an city lies within the South Central Shandong geothermal area, encompassing Taishan-Daidao'an, Feicheng-Anjiazhuang, and Daiyue geothermal fields (Tan et al. 2019; Cao et al. 2018; Kang et al. 2022; Zheng et al. 2023). This region is characterized by convective belt-like geothermal reservoir wtih shallow burial depths, fault-controlled structures, and higher geothermal gradients beneath surface layers (Cai et al. 2015; Tan et al. 2019; Mao et al. 2019; Liu et al. 2020). Geothermal resources in Tai'an offer rich potential due to their high water temperature and are abundant water supply. Current exploitation models focus on bathing, recuperation, agriculture, and aquaculture (Li et al. 2020; Meng et al. 2021; Li et al. 2021). The city's 14th Five-Year Plan for Energy Development emphasizes optimizing hydrothermal geothermal use, including water-source heat pump systems leveraging sewage and mine water resources. Despite growing utilization of the geothermal resources, scaling and corrosion hinder efficient exploitation. This study targets geothermal water in Tai'an main fields (Taishan-Daidao'an, Feicheng-Anjiazhuang, and Daiyue), employing geochemical simulations, Ryznar Index, and other evaluations to predict the corrosion and scaling trends and propose solutions to mitigate scaling and corrosion, enhancing resource efficiency.

1 Geological conditions

The geothermal fields in Tai'an City comprise the Daidao'an geothermal field, Feicheng-Anjiazhuang geothermal field, and Daiyue-Qiaogou geothermal field, all located within the central uplift in Shandong Province. As shown in Fig. 1(a) and Fig. 1(b), these fields are predominantly located at the intersections of uplifts and depressions, where the influence of faults is notable. Deep and extensive faults act as conduits for heat from deep sources, while atmospheric precipitation percolates throughrock fissures and heat-controlling faults. This enables deep circulation and thermal energy exchange under the influence of regional hydraulic head pressures. The resulting ascends to shallow depths and accumulated within structural faults to form geothermal reservoirs. These geothermal fields are characterized by relatively small distribution areas, shallow burial depths, high geothermal gradients beneath the covering layers, typical of convective belt-like geothermal reservoir (Mou, 2017; Wang et al. 2020; Gao et al. 2023).

The Taishan Daidao'an geothermal field, located in Daidao'an Village, Tai'an City, is a deep-circulating convective, belt-like geothermal reservoir positioned at the convergence of the Tailai Depression and the Mount Tai Uplift. The field features highly developed fault structures, prominently the Mount Tai Fault and the Daidao'an Fault. The reservoir layers predominantly consist of oolitic limestone of the Zhangxia Formation and chert nodule limestone of the Cambrian Zhushadong Formation, buried at depths of 200–800 m. The Feicheng Anjiazhuang geothermal field, located in Anjiazhuang, Feicheng, Tai'an City, lies at the intersection of the Wenkou Depression and the Bushan Uplift. Its reservoir layers, within the Cambrian Zhushadong Formation, are predominantly composed of dolomite, dolomitic limestone and marl. These layers are buried at depths of 10 m–400 m, with a geothermal gradient of 3.0°C/100 m–8.58°C/100 m. The Qiaogou geothermal field, situated in Qiaogou Village, Zoulai Town, Tai'an City, lies at the intersection of the Tailai Depression and the Xinfu Mountain Uplift. Its main reservoir layer consists of Neoarchean granodiorite, with a top plate buried at a depth of approximately 10 m. The reservoir temperature is 20°C–41.4°C, and its water inflow capacity is 120 m^3/d–480 m^3/d.

2 Sample collection and calculation methods

2.1 Sample collection

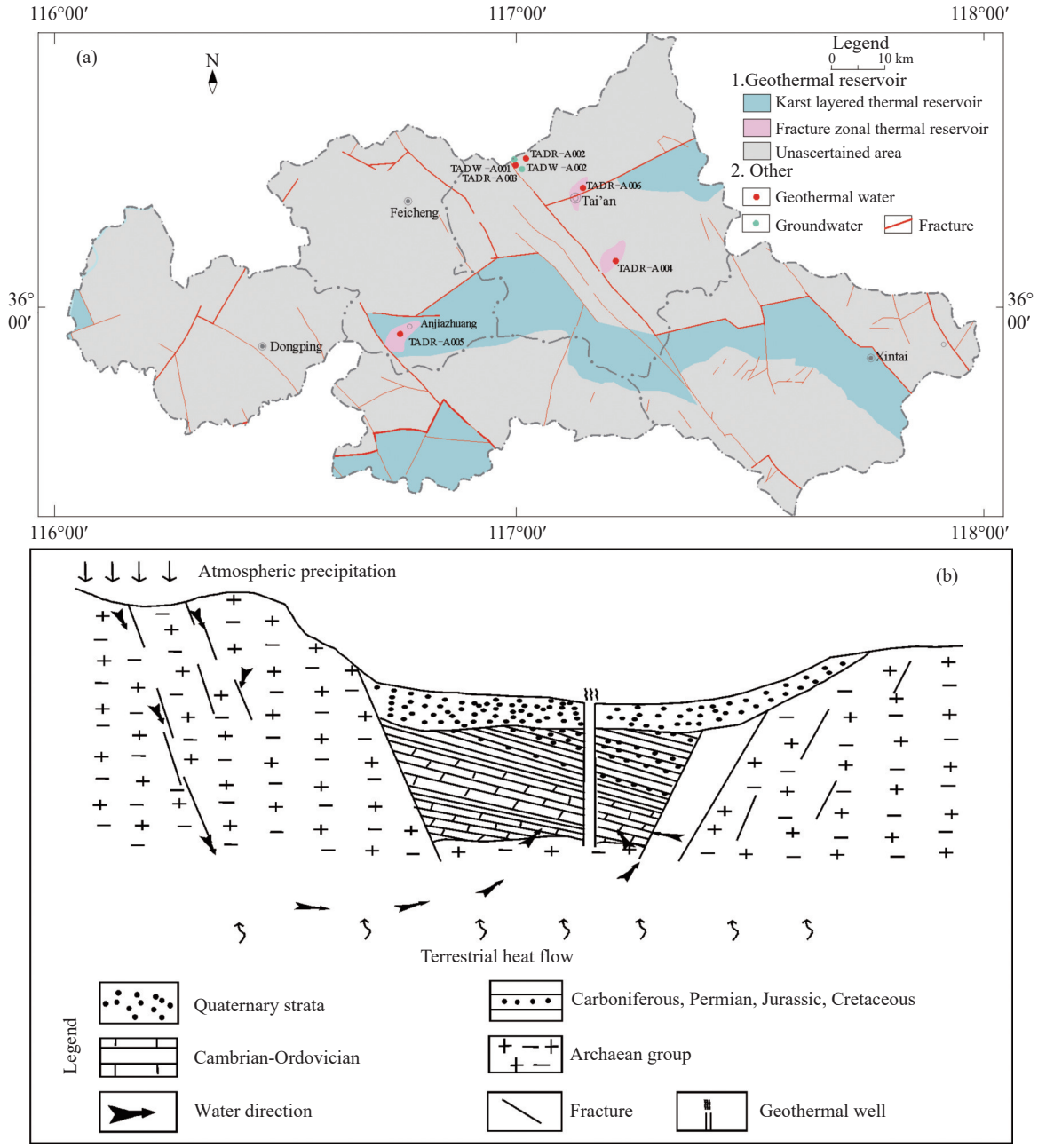

Fig. 1 Distribution of geothermal resources and sampling point (a) and the conceptual model of geothermal system (b) in Tai'an

In this study, a total of five sets of geothermal water samples were collected: One from the Qiaogou geothermal field (TADR-004), one from the Anjiazhuang geothermal field (TADR-005), and one from the Daidao'an geothermal field (TADR-006). The remaining two sets were obtained from geothermal fields situated at the foot of Mount Tai in the north of Tai'an City (TADR-002 and TADR-003). See Fig. 1(a) for the sampling locations.

Field measurements of pH and temperature were conducted using handheld testing devices. For comprehensive water quality analysis, 2.5 L polyethylene plastic buckets were used to collect the samples. These samples were dispatched to the Key Laboratory of Groundwater Sciences and Engineering, Ministry of Natural Resources, for water quality analysis. This analysis adhered to the GB/T 8538—2008 National Standard for Testing Natural Mineral Water. During the test process, cations such as K^+, Na^+, Ca^{2+}, Mg^{2+} were quantified using the Inductively Coupled Plasma (ICP) method, while anions like HCO_3^-, Cl^-, SO_4^{2-}, and F^- were analyzed through ion chromatography. The balance error between anions and cations was controlled within 3%.

2.2 Calculation method

The hydrochemical data analysis in this study employed the Schukalev classification method to determine hydrochemical types. Software tools including SPSS, Aquachem (for hydrochemical type analysis), PHREEQC (for saturation index calculation), and Excel were utilized for analyzing the hydrochemical data. To quantitatively assess the corrosion and scaling trends of geothermal water, a range of index methods were employed, including the corrosion coefficient, Ryznar Index, Larson Index, total amount of boiler scale evaluation, and hard fouling evaluation.

1) Total boiler scale evaluation (H_0)

The total amount of boiler scale (H_0) was calculated using:

$$H_0 = S + \rho + 36r(Fe^{2+}) + 17r(Al^{3+}) + 20r(Mg^{2+}) + 59r(Ca^{2+}) \quad (1)$$

Where: S is suspended matter content in geothermal water (mg/L); ρ *is C* (colloid content) = $SiO_2 + Fe_2O_3 + Al_2O_3$ (mg/L).

Judgment criteria:

H_0< 125: Geothermal water with little scaling;

125≤H_0<250: Geothermal water with a little scaling;

250≤H_0<500: Geothermal water with abundant scaling;

H_0≥500: Geothermal water with significant scaling.

2) Calcium carbonate scaling

a) For chloride ion content ≥ 25 mol%, the Larson Index (LI) can be used to assess scaling tendency and corrosion of calcium carbonate:

$$\mathrm{LI} = \frac{\rho(Cl^-) + \rho(SO_4^{2-})}{ALK} \quad (2)$$

Where: $\rho(Cl^-)$ is chlorides concentration (mg/L); $\rho\left(SO_4^{2-}\right)$ is sulfate concentration (mg/L); *ALK* is total alkalinity as $CaCO_3$ (mg/L).

Judgment criteria:

LI≥0.5: Non-scaling, corrosive;

0.5≤LI<3.0: Slightly corrosive;

3.0≤LI<10.0: Highly corrosive;

LI<0.5: Scaling potential, no corrosive.

For this study, chloride ion content was below 25 mol%, so this method was not applied.

b) For chloride ion content <25 mol%, the Ryznar Index (*RI*) was used:

$$RI = 2\mathrm{pH_s} - \mathrm{pH_a} \quad (3)$$

$$\mathrm{pH_a} = -lgc(Ca^{2+}) - lg(\mathrm{ALK}) + K_e \quad (4)$$

Where: $\mathrm{pH_S}$ is calculated pH; $\mathrm{pH_a}$— measured pH; $c(Ca^{2+})$ is calcium concentration; ALK is total alkalinity as HCO_3^-; K_e: is a constant (1.8–2.6, dependent on total dissolved solids and water temperature).

Judgment criteria:

RI<4.0: Very severe scaling;

4.0≤*RI*<5.0: Severe scaling;

5.0≤*RI*<6.0: Moderate scaling;

6.0≤*RI*<7.0: Slight scaling;

RI>7.0: Non-scaling.

3) Calcium sulfate scaling

For water temperature < 100°C, calcium sulfate precipitates as dihydrate gypsum ($CaSO_4 \cdot 2H_2O$). The $CaSO_4$ scaling is assessed using the R.S index:

$$R.S = 10^{(\log ppmCa^{2+} + \log ppmSO_4^{2-} - \log K)} \quad (5)$$

Where: K is a constant related to temperature and total dissolved solids.

Judgment criteria:

R.S<1: No scaling;

R.S>1: Scaling potential.

4) Hard fouling evaluation

The hard fouling coefficient K_n was calculated:

$$K_n = H_n / H_o \quad (6)$$

$$H_n = SiO_2 + 20r(Mg^{2+}) + 68\,[r(Cl^-) + r(SO_4^{2-}) - r(Na^+) - r(K^+)] \quad (7)$$

Where: H_o is total amount of boiler scale (mg/L); r is milligram equivalents per liter of ion content

Judgment Criteria:

K_n<0.25: Soft sediment;

0.25≤K_n≤0.5: Moderate sediment;

K_n>0.5: Hard sediment.

5) Corrosion evaluation

Corrosion coefficient (K_k) can be used to evaluate the corrosivity of geothermal water.

For acidic water:

$$K_K = 1.008[r(H^+) + r(Al^{3+}) + r(Fe^{2+}) + r(Mg^{2+}) - r(HCO_3^-) - r(CO_3^{2-})] \quad (8)$$

For alkaline water:

$$K_K = 1.008[r(Mg^{2+}) - r(HCO_3^-)] \quad (9)$$

Where: r is milligram equivalent concentration of ions (meq/L).

Judgment Criteria:

K_k>0: Corrosive;

K_k<0 and K_k+0.0503Ca^{2+}>0: Semi-corrosive;

K_k<0 and K_k+0.0503Ca^{2+}<0: Non-corrosive.

6) Foaming evaluation

The foaming coefficient F was calculated:

$$F = 62r(Na^+) + 78r(K^+) \quad (10)$$

Where: $r(Na^+)$, $r(K^+)$: Ion content (mg/L).

Judgement Criteria:

F<60: Non-foaming;

60≤*F*≤200: Semi-foaming;

F>200: Foaming.

3 Results and discussion

3.1 Hydrochemical characteristics of geothermal water

In the study area, the geothermal water temperatures ranged from 25°C to 69°C, with pH values between 7.13 and 8.1 (Table 1). Notably, the Total Dissolved Solids (TDS) value of the geothermal water sample from Anjiazhuang, Feicheng reached 2,240 mg/L, while samples from other areas exhibited TDS values ranging from 455 mg/L to 940 mg/L. Hydrochemical analyses were performed using a Piper diagram (Fig. 2), Schoeller diagram (Fig. 3), and major ion percentages (Fig. 4).

The findings reveal that Na^+ and Ca^{2+} are the primary cations, while SO_4^{2-} and HCO_3^- are the main anions. Hydrochemical types identified include Na-Ca-SO_4, Ca-Na-SO_4-HCO_3, Na-Ca-SO_4-Cl-HCO_3, Na-Ca-SO_4-Cl, and Ca-Na-Mg-SO_4-HCO_3. Concentrations of Na^+, K^+, Ca^{2+}, Cl^-, and SO_4^{2-} in geothermal water surpass those in surface water and shallow groundwater due to prolonged pathways, enhanced water-rock interactions, and higher geothermal reservoir temperatures. Conversely, Mg^{2+} level is generally lower in geothermal water than in shallow groundwater, likely due to cation exchange and adsorption processes at elevated temperatures. The concentrations of bicar-

Table 1 Statistics of chemical components of geothermal water in Tai'an

Descriptive statitics	pH	T/°C	Ion index content/ mg·L^{-1}														
			TDS	H_2SiO_3	K^+	Na^+	Ca^{2+}	Mg^{2+}	Li^+	Sr^{2+}	Cl^-	SO_4^{2-}	HCO_3^-	NO_3^-	F^-	Mn	Ba
Minimum value	7.13	25.00	455.00	18.20	2.27	45.70	72.95	6.13	0.03	0.65	26.57	156.50	80.36	0.00	0.51	0	0
Maximum value	8.10	69.00	2,240.64	65.77	17.75	450.00	218.84	30.63	0.52	7.00	309.79	1,052.72	194.36	25.56	4.0	0.12	0.077
Mean value	7.78	44.00	1,029.76	43.74	7.49	174.76	113.42	13.79	0.18	3.57	110.99	447.56	132.36	9.71	2.164	0.057	0.072
Median	8.10	41.00	836.04	42.41	5.70	154.10	85.29	8.04	0.11	2.86	60.67	292.58	119.10	9.38	1.86	0.05	0.072

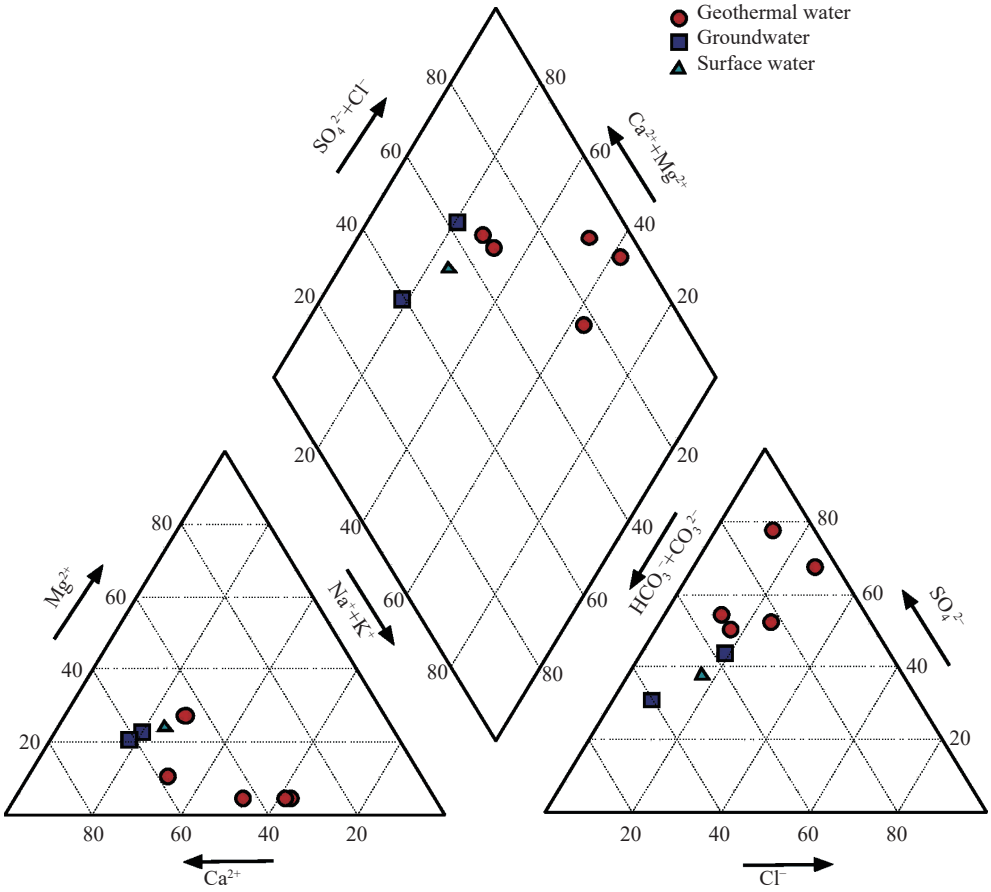

Fig. 2 Piper diagram of water sample in Tai'an

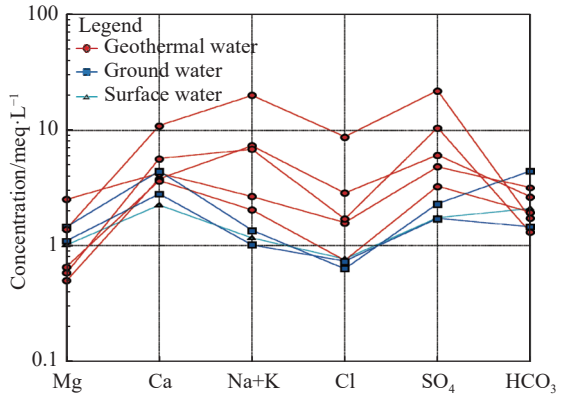

Fig. 3 Schoeller diagram of water sample in Tai'an

bonate ions in geothermal water exhibit minimal variation compared to shallow groundwater and surface water and show weak correlation with other ions.

The SPSS analysis revealed a significant positive correlation between Cl^- and K^+, Na^+, Ca^{2+}, SO_4^{2-}, and TDS (Table 2). A strong correlation between Na^+ and Cl^- suggests a shared origin, possibly the dissolution of rock salt or other deep-seated minerals. In the study of groundwater hydrochemistry evolution, the equivalent ratio of cations $r(Na^+)/r(Cl^-)$ provides a better indicator of cation exchange process. As shown in Fig. 5, the equivalent ratios of geothermal water are greater than 1, indicating relatively strong cation exchange reactions.

The chlor-alkali indices CAI1 and CAI2 further illustrate the likelihood of these cation exchange reactions (Fig. 6). When Na^+ and K^+ in the water exchange with adsorbed Ca^{2+} and Mg^{2+}, CAI1 and CAI2 values are positive. Conversely, when Ca^{2+} and Mg^{2+} exchange with adsorbed Na^+ and K^+, CAI1 and CAI2 values become negative. The magnitude of the absolute values of CAI1 and CAI2 reflects the intensity of the exchange reactions. It can be seen from the figure that the indices for the geothermal water are negative with large absolute values, consistent with the earlier analysis, confirming that cation exchange reactions are indeed relatively strong.

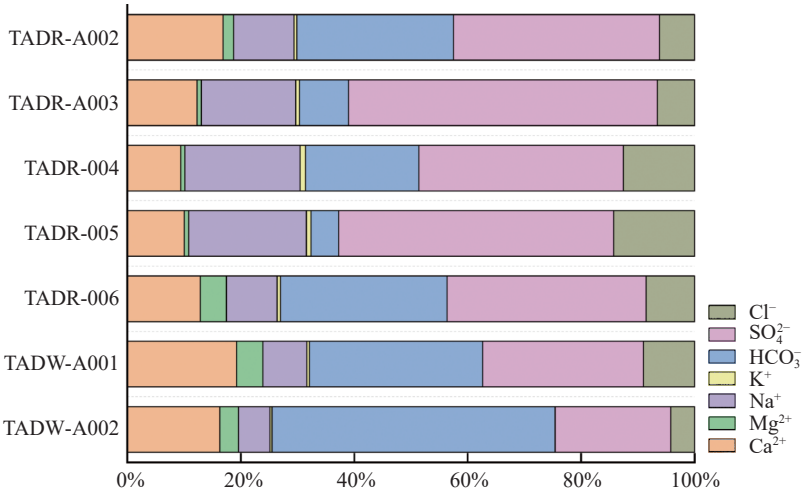

Fig. 4 Major ions percentage of the water samples in Tai'an represented by bar graph

Table 2 Correlation coefficient of geothermal water in Tai'an

	K^+	Na^+	Ca^{2+}	Mg^{2+}	Cl^-	SO_4^{2-}	HCO_3^-	TDS	pH
K^+	1								
Na^+	0.992**	1							
Ca^{2+}	0.928*	0.950*	1						
Mg^{2+}	0.051	−0.016	0.15	1					
Cl^-	0.992**	0.980**	0.940*	0.129	1				
$SO4_{2-}$	0.946*	0.971**	0.988**	0.054	0.938*	1			
HCO_{3-}	−0.287	−0.402	−0.458	0.611	−0.248	−0.499	1		
TDS	0.982**	0.988**	0.981**	0.115	0.982**	0.986**	−0.37	1	
pH	0.559	0.464	0.349	0.521	0.547	0.371	0.56	0.48	1

Notes: **: Significant correlation at the 0.01 level (two-tailed); *: Significant correlation at the 0.05 level (two-tailed).

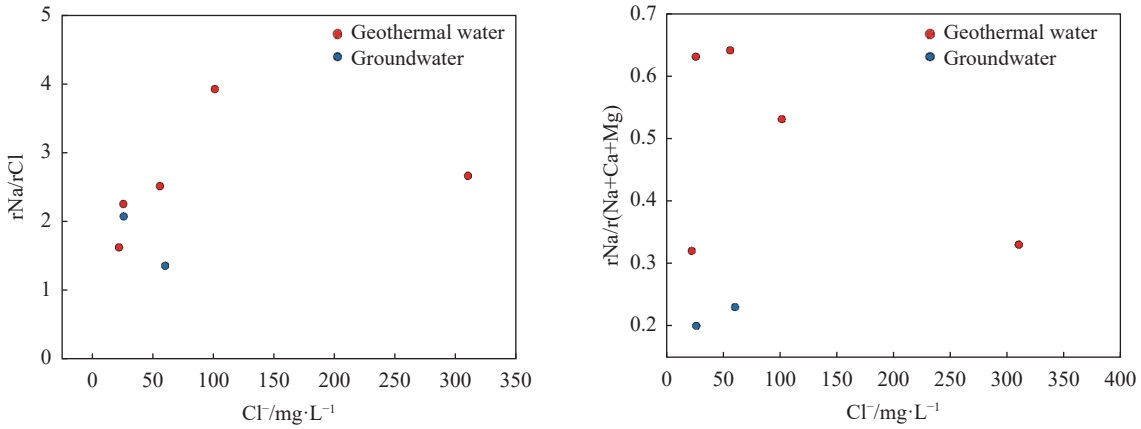

Fig. 5 Plot of the ratio relationships between Cl^- and rNa^+/rCl^- and $rNa^+/r(Na^+{+}Ca^{2+}{+}Mg^{2+})$ in the samples

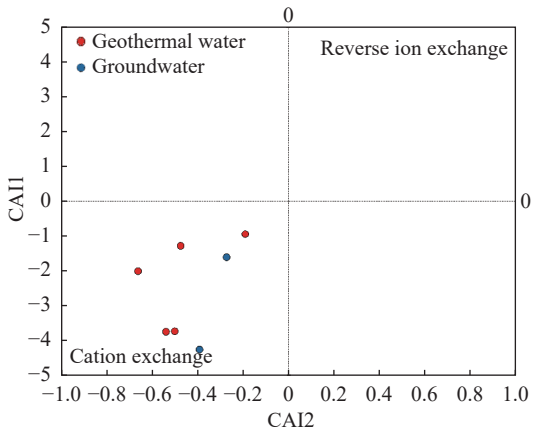

Fig. 6 Relationship between CAI1 and CAI2 in geothermal water samples

The hydrogeochemical processes governing the formation of major ions in hot water predominantly involve the dissolution and precipitation of carbonate, sulphate, and silicate minerals. As illustrated in the Fig. 7, geothermal water in the study area closely aligns with the $2[Ca^{2+}] = [HCO_3^-]$ line, with a slight inclination towards the $[Ca^{2+}]$ side. This suggests that the Ca^{2+} and HCO_3^- ions in geothermal water predominantly originate from the dissolution of carbonate minerals like calcite and dolomite. The tendency towards the Ca^{2+} side suggests additional dissolution of silicate minerals like feldspar. The $[Mg^{2+}]/[Ca^{2+}]$ ratio in geothermal water is consistently below 1, signifying a limited influence of magnesium-deficient minerals like calcite on the hydrochemical composition of deep geothermal water. Similarly, the $[Na^+]/[Ca^{2+}]$ ratio remains relatively low, approximating $[Na^+]/[Ca^{2+}] = 1$, further indicating a minimal contribution of silicate minerals dissolution to the water's composition. Additionally, the $[Ca^{2+}+Mg^{2+}]$-$[HCO_3^-+SO_4^{2-}]$ diagram provides insight into the hydrogeochemical processes affecting the primary chemical components of geothermal water. The observed ratio of $[Ca^{2+}+Mg^{2+}]/[HCO_3^-+SO_4^{2-}]$ approximates 1 (Fig. 8), indicating that the precipitation-dissolution equilibrium of carbonate, silicate, and sulfate minerals collectively influences the composition of geothermal water. However, the relatively minor role of silicate mineral dissolution supports that the reservoirs are

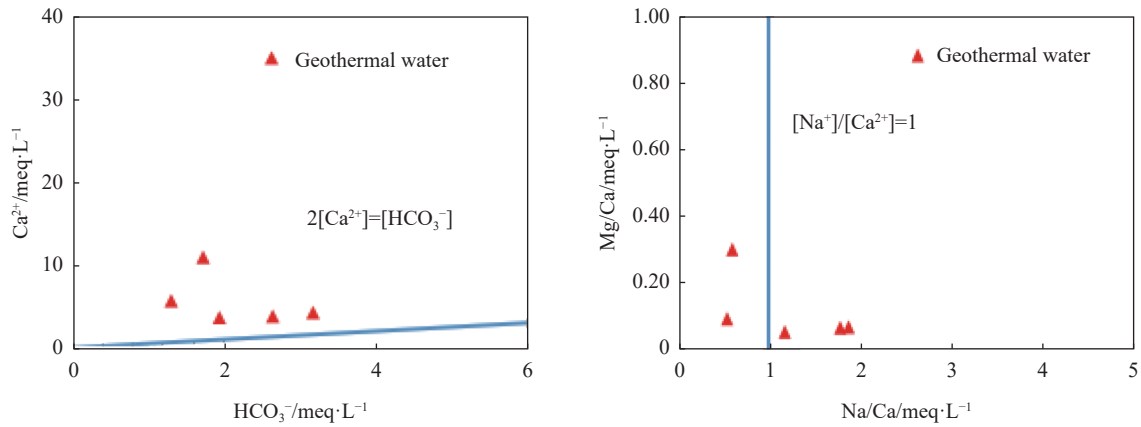

Fig. 7 Comparison of ion concentration in geothermal water (Ca^{2+}–HCO_3^-, $[Mg^{2+}]/[Ca^{2+}]$–$[Na^+]/[Ca^{2+}]$)

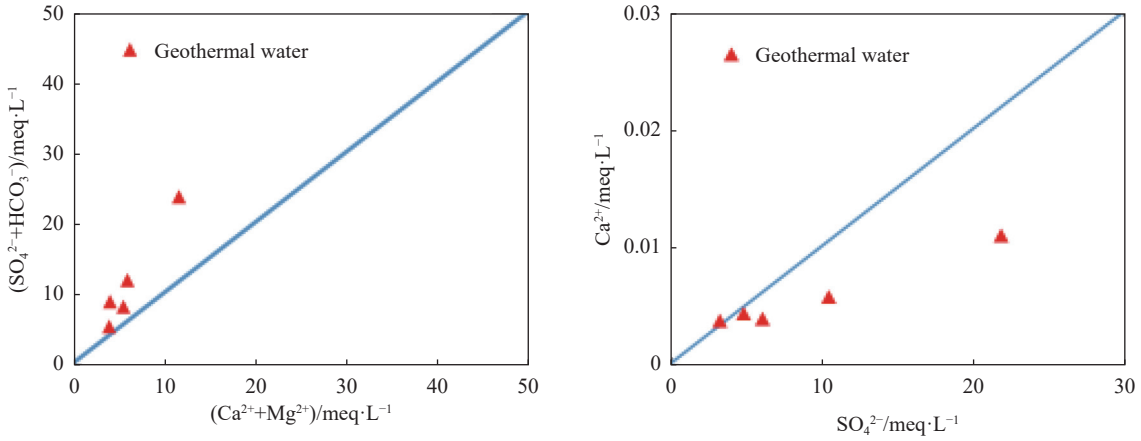

Fig. 8 Comparison of ion concentration in geothermal water ($(Ca^{2+} + Mg^{2+})$–$(HCO_3^- + SO_4^{2-})$, Ca^{2+}–SO_4^{2-})

predominantly affected by the precipitation-dissolution dynamics of carbonate and sulfate minerals.

3.2 Hydrogeochemical simulation of scaling mechanism and the saturation index

To further analyze the predominant scaling type and its tendencies, hydrogeochemical modeling (Aquachem) was conducted to simulate the saturation state of geothermal water. The mineral Saturation Index (*SI*) (Oddo et al. 2021; Stahl et al. 2000) was used, which is defined as:

$$SI = \lg \frac{IAP}{K} \tag{11}$$

Where: K is the equilibrium constant for the mineral dissolution reaction; IAP represents the activity product of the relevant ions in the mineral dissolution reaction. Positive *SI* values indicate supersaturation (precipitation tendency), while negative *SI* values suggest undersaturation (dissolution tendency).

The geochemical simulation results (Figs. 9 and 10) reveal that carbonate scaling is the dominant type in the study area. Sulfate scaling is minimal, and appearing only at sampling points TADR-A002 and TADR-A003, and silicate scaling occurs marginally at 100°C. The moderate to low-temperature nature of the geothermal water supports the predominance of carbonate scaling.

3.3 Corrosion and scaling analysis

Given that chloride ion concentrations remain below 25%, the Larson Index (*LI*) is inapplicable

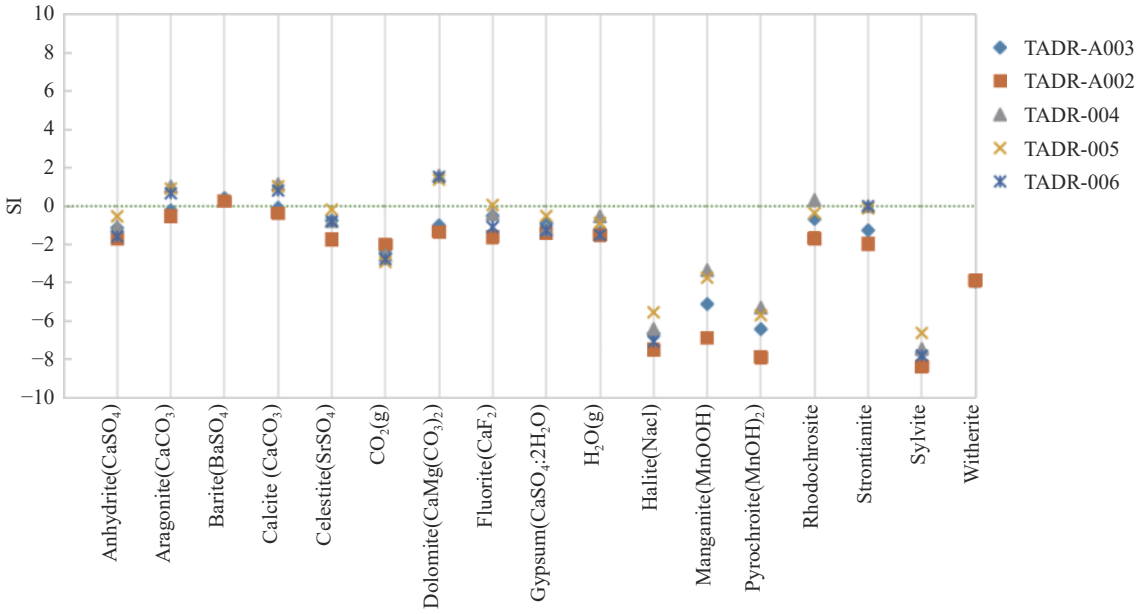

Fig. 9 The figure of geothermal water minerals Saturation Index

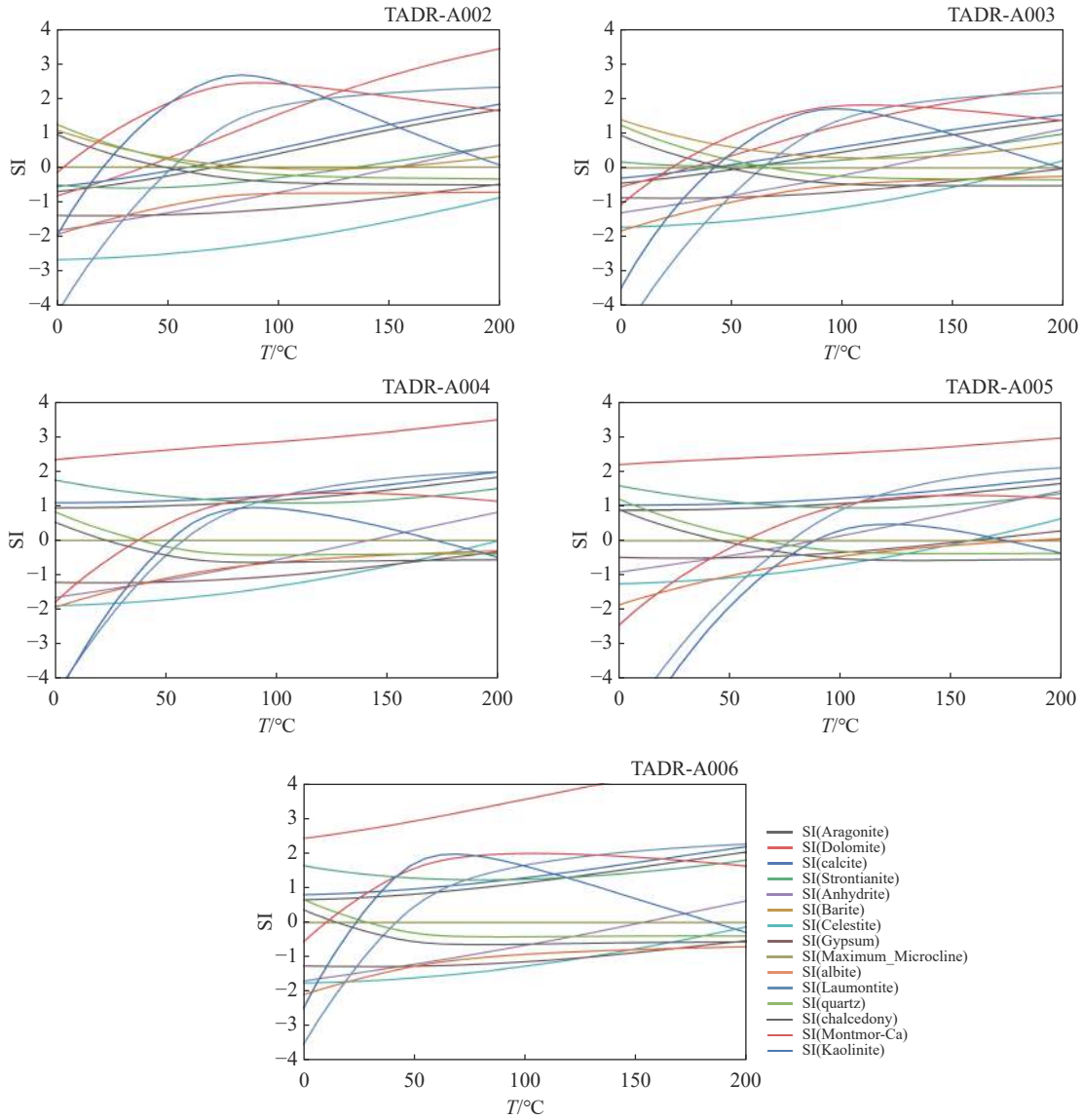

Fig. 10 The relationship between minerals saturation index and temperature

for calcium carbonate scaling and corrosion assessment. Instead, the corrosion coefficient (K_k) and Ryznar Index (*RI*) were used, alongside evaluations for hard fouling and foaming (Table 3 and Fig. 11). The findings indicate no calcium sulfate scaling, consistent with the saturation index analysis. However, all samples exhibit calcium carbonate scaling. Specifically, geothermal water samples from Nanmatao Village and Qiaogou Wuyue Wenquan in Daiyue District are classified as non-corrosive, while those from Shila Village shows moderate corrosive property. Samples from Anjiazhuang in Feicheng and Wenquan Road in Taishan District are deemed corrosive. Based on the *RI* assessment, calcium carbonate scaling varies, with slight scaling in Nanmatao Village and Shila Village, while the total amount of scaling is higher. The remaining three geothermal water samples exhibit moderate scaling. According to the evaluation of total amount of boiler scale, geothermal water sample from Anjiazhuang in Feicheng has a significant amount of scaling at 724.26 mg/L, while others range from 256.66 mg/L to 380.27 mg/L; Hard sediments are present in all geothermal water samples. Water samples from Nantao Village and Wenquan Road in Taishan District are classified as semi-foaming, whereas those from other areas are identified as foaming water. Remarkably, the geothermal water from Anjiazhuang in Feicheng demonstrates the highest foaming coefficient, significantly surpassing other geothermal water samples. Overall, the geothermal water sample from Anjiazhuang in Feicheng demonstrate the highest level of corrosion, scaling, and foaming, significantly exceeding those of the other regions.

Table 3 Evaluation results of water samples in Tai'an

Classification	Numbering	Location	Water temperature	pH	Corrosion evaluation (K_k)			Evaluation of calcium carbonate scaling (RI)	
					K_k	K_k+0.0503 Ca^{2+}	Judgement	Calculated result	Evaluation result
Geothermal water	TADR-A002	Xingyuan, Nanmatao Village, Tai 'an City	25	7.13	−0.64	−0.27	Non-corrosive water	6.84	Slight scaling
	TADR-A003	North of Shila Village, Tai 'an City	30	7.45	−0.14	0.43	Semi-corrosive water	6.61	Slight scaling
	TADR-004	Qiaogou Wuyue Wenquan, Daiyue District, Tai'an City	69	8.10	−1.66	−1.28	Non-corrosive water	5.67	Moderate Scaling
	TADR-005	East of Dongzhaocun Villiage, Feicheng, Anjiazhuang, Tai 'an City	52	7.90	1.06	\	Corrosive water	5.71	Moderate Scaling
	TADR-006	Wenquan Road, Taishan District, Tai'an City	\	8.05	1.85	\	Corrosive water	5.42	Moderate Scaling
Cold groundwater	TADW-A001	Nanmatao Village, Tai'an City	18	6.74	0.77	\	Corrosive water	7.68	Non-scaling
	TADW-A002	Foyu Village, Taohuayu Town, Tai'an City	20	7.21	−1.53	−1.09	Non-corrosive water	5.88	Moderate scaling

Table 3 (continued)

Classification	Numbering	Location	Evaluation of calcium sulfate scaling (R.S)		Evaluation of total amount of boiler scale (H_0)		Evaluation of hard fouling		Foaming evaluation	
			Calculated result	Evaluation result	Calculated result	Evaluation result	Calculated result	Evaluation result	Calculated result	Evaluation result
Geothermal water	TADR-A002	Xingyuan, Nanmatao Village, Tai 'an City	0.006	Non-scaling	279.21	Abundant scaling	1.55	Hard sediment	128.06	Semi-foaming
	TADR-A003	North of Shila Village, Tai 'an City	0.030	Non-scaling	380.27	Abundant scaling	2.98	Hard sediment	427.10	Foaming
	TADR-004	Qiaogou Wuyue Wenquan, Daiyue District, Tai'an City	0.012	Non-scaling	256.66	Abundant scaling	9.02	Hard sediment	460.82	Foaming
	TADR-005	East of Dongzhaocun Villiage, Feicheng, Anjiazhuang, Tai 'an City	0.111	Non-scaling	724.26	Significant scaling	10.58	Hard sediment	1249.65	Foaming
	TADR-006	Wenquan Road, Taishan District, Tai'an City	0.011	Non-scaling	316.99	Abundant scaling	5.27	Hard sediment	167.13	Semi-foaming
Cold groundwater	TADW-A001	Nanmatao Village, Tai'an City	0.003	Non-scaling	215.09	A little scaling	1.33	Hard sediment	63.72	Semi-foaming
	TADW-A002	Foyu Village, Taohuayu Town, Tai'an City	0.005	Non-scaling	319.99	Abundant scaling	1.10	Hard sediment	85.12	Semi-foaming

4 Conclusions

(1) The geothermal fields in Tai'an, including the Taishan Daidao'an, the Feicheng Anjiazhuang, and

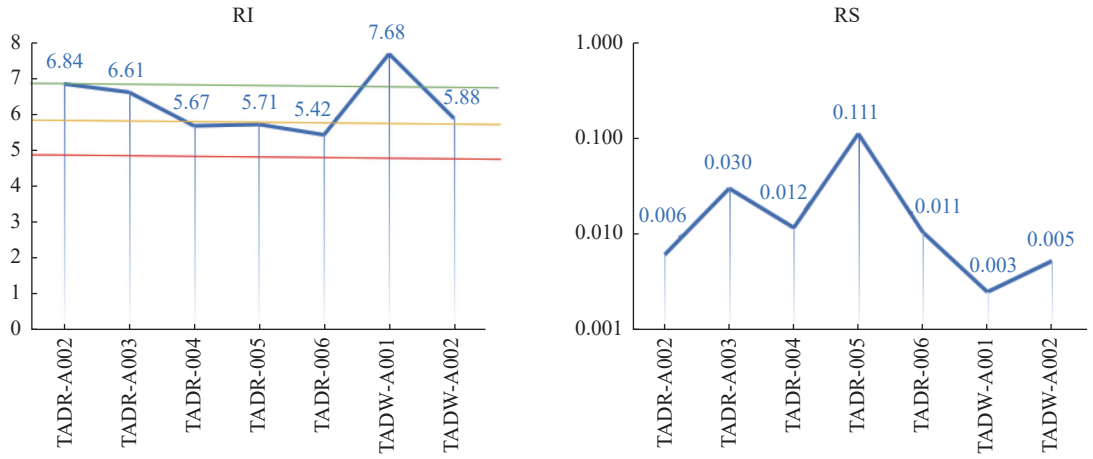

Fig. 11 RI and R.S values for different fluids in the study area

the Daiyue geothermal fields, are classified as fracture geothermal reservoirs. The predominant hydrochemical types are Na-Ca-SO_4 and Ca-Na-SO_4-HCO_3, with pH levels ranging from 7.13 to 8.1, indicating weakly alkaline water. Simulations reveal that scaling tendencies are predominantly influenced by calcium carbonate.

(2) Due to low chloride levels (<25%) in all geothermal water samples, the Larson index (LI) is not suitable for evaluating corrosion and scaling trends. Corrosion is instead evaluated using the Corrosion coefficient (Kk), while scaling tendencies are assessed with the total amount of boiler scale evaluation, the Ryznar Index (RI) and the hard scale coefficient (K_n). The results reveal that the geothermal water of Daiyue Qiaogou geothermal field is corrosive bubble water, moderate calcium carbonate scaling, and abundant boiler scaling. The geothermal water of Feicheng Anjiazhuang geothermal field is non-corrosive bubble water, moderate calcium carbonate scaling, and significant boiler scaling. The geothermal water of Daidao'an geothermal field is corrosive semi-bubble water, moderate calcium carbonate scaling, and abundant boiler scaling.

(3) Corrosion and scaling are widespread in geothermal water across the study area. the Feicheng Anjiazhuang geothermal field exhibits the highest levels of corrosion, scaling, and foaming compared to other regions. Therefore, anti-corrosion measures, scale inhibitors, and passivation agents should be implemented to enhance the efficiency of geothermal development and utilization.

Acknowledgements

This research was funded by the Key R&D Program of Henan, China (No. 241111321000) and China Geological Survey Program (DD20221676).

References

Appelo CAJ, Postma D. 2005. Geochemistry, groundwater and pollution. Rotterdam: A.A. Balkema Publisher.

Arteaga CC, Rodríguez JA, Clemente CM, et al. 2013. Estimation of useful life in turbines blades with cracks in corrosive environment. Engineering Failure Analysis, 35: 576−589. DOI：10.1016/j.engfailanal.2013.05.013.

Cao YL, Cheng GJ, Zhao CL, et al. 2018. Application of CSAMT in hydrogeology exploration in Shandong Province—An example from geothermal exploration in Changdao County (south four islands). Journal of Groundwater Science and Engineering, 6(1): 58−64. DOI：10.19637/j.cnki.2305-7068.2018.01.00.

Cai YX, Zhong XY. 2015. Brief introduction to typical geothermal field in South Region of Shandong Province. Shandong Land and Resources, 31(5): 24−30. (in Chinese)

Cen JW, Jiang F. 2022. Geothermal well scaling simulation by combining two phase flow with chemical equilibrium. Advances in New and Renewable Energy, 10(1): 20−26. (in Chinese)

Delalande M, Bergonzini L, Gherardi F, et al. 2011. Fluid geochemistry of natural manifestations from the Southern Poroto–Rungwe hydrothermal system (Tanzania): Preliminary

conceptual model. Journal of volcanology and geothermal research, 199(1/2): 127−141. DOI：10.1016/j.jvolgeores.2010.11.002.

Florent B, Christelle M, Elisabeth G, et al. 2000. Hydrochemical and isotopic characterisation of the Bathonian and Bajocian coastal aquifer of the Caen area (northern France). Applied geochemistry, 15(6): 791−805. DOI：10.1016/S0883-2927(99)00088-8.

Gallup DL. 2009. Production engineering in geothermal technology: A review. Geothermics, 38(3): 326−334. DOI：10.1016/j.geothermics.2009.03.001.

Gao NA, Wang XW, Liang HJ, et al. 2023. Genetic mechanism of geothermal system in Daming Sag, Linqing Depression in the junction of Hebei, Shandong and Henan Provinces and its exploration potential. Geology in China, 50(4): 1149−1162. (in Chinese) DOI：10.12029/gc20201230002.

He YJ, Liu X, Xing LX, et al. 2022. Scaling process simulation and anti-scaling measures in karst geothermal field in Baoding, Hebei. Earth Science Frontiers, 29(4): 430−437. (in Chinese) DOI：10.13745/j.esf.sf.2021.11.4.

Kang FX, Yang XC, Wang XP, et al. 2022. Hydrothermal features of a sandstone geothermal reservoir in the North Shandong Plain, China. Lithosphere, 2021(Special 5): 1675798. DOI：10.2113/2022/1675798.

Langelier WF. 1946. Chemical equilibria in water treatment. Journal (American Water Works Association), 38(2): 169−178.

Larson TE, Sollo FW. 1967. Loss in water main carrying capacity. Journal (American Water Works Association), 59(12): 1565−1572. DOI：10.1002/j.1551-8833.1967.tb03486.x.

Lei HW, Bai B, Cui YX, et al, 2023. Quantitative assessment of calcite scaling of a high temperature geothermal production well: Hydrogeochemistry—Application to the Yangbajing geothermal fields, Tibet. Earth Science, 48(3): 935–945. (in Chinese) DOI：10.3799/dqkx.2022.163.

Li HQ, Zhang SS, Xie MZ, et al. 2020. The occurrence characteristics and exploration and development direction of geothermal resources in Yuxian Basin, northwest Hebei Province. Geological Review, 66(4): 919−932. (in Chinese) DOI：10.16509/j.georeview.2020.04.010.

Li XL, Du ZW, Zhang L,et al. 2021. Distribution characteristics and present condition of exploitation and utilization of geothermal resources in Shandong Province. Shandong Land and Resources, 37(1): 37−43. (in Chinese) DOI：10.12128/j.issn.l672 6979.2021.01.005.

Liang HJ, Guo XF, Gao T, et al. 2020. Scaling spot prediction and analysis of influencing factors for a geothermal well in Boye County, Hebei Province. Petroleum Drilling Techniques, 48(5): 105−110. (in Chinese) DOI：10.11911/syztjs.2020096.

Lin HB. 2022. Study on scaling mechanism and anti-scaling of high temperature geothermal wellboree. Xi'an Shiyou University, (in Chinese)

Liu MY. 2015. A review on controls of corrosion and scaling in geothermal fluids. Advances in New and Renewable Energy, 3(1): 38−46. (in Chinese) DOI：10.3969/j.issn.2095-560X.2015.01.007.

Liu YQ, Zhou L, Lv L, et al. 2020. Geothermal geological characteristics and genesis of hot water in the central mountain area of Shandong Province. Geological Bulletin of China, 39(12): 1908−1918. (in Chinese)

Lv Y. 2020. Preparations and properties in pool boiling of anticorrosion and antifouling coatingson different metal substrates for oilfield geothermal water. Tianjin University. (in Chinese)

Mao XP, Li KW, Wang XW. 2019. Causes of geothermal fields and characteristics of ground temperature fields in China. Journal of Groundwater Science and Engineering, 7(1): 15−28. DOI：10.19637/j.cnki.2305-7068.2019.01.002.

Manan S, Vrutang S, Kaushalkumar D, et al. 2023. Evaluation of geothermal water and assessment of corrosive and scaling potential of water samples in Tulsishyam Geothermal Region, Gujarat, India. Environmental Science and Pollution Research, 30(15):

44684−44696. DOI：10.1007/s11356-023-25165-8.

Marimuthu S, Reynoids DA, La Salle CLG, et al. 2005. A field study of hydraulic, geochemical and stable isotope relationships in a coastal wetlands system. Journal of hydrology, 315(1/4): 93−116. DOI：10.1016/j.jhydrol.2005.03.041.

Meng XL, Wang QB, Yang PJ. 2021. Investigation and problem analysis on development and utilization of geothermal resources in Shandong Province. Shandong Land and Resources, 37(11): 36−42. (in Chinese) DOI：10.12128/ji.ssn.1672 6979.2021.11.006.

Mou LK. 2017. Study of occurrence characteristics and formation model of geothermal water in Shandong Province. College of Earth Science and Engineering. (in Chinese)

Oddo JE, Tomson MB. 1994. Why scale forms in the oil field and methods to predict it. SPE Production & Facilities, 9: 47–54. DOI：10.2118/21710-PA.

Pang Y. 2023. Study on the corrosion mechanism of abandoned oil wells to geothermal wells-Takingan oil well in the western oil region of Northern Shaanxias–An example speciality: Petroleum and Natural Gas. Xi'an Shiyou University. (in Chinese)

Pátzay G, Stáhl G, Karman FH, et al. 1998. Modeling of scale formation and corrosion from geothermal water. Electrochimica Acta, 43(1): 137−147. DOI：10.1016/S0013-4686(97)00242-9.

Pazheri FR, Othman MF, Malik NH. 2014. A review on global renewable electricity scenario. Renewable and Sustainable Energy Reviews, 31(3): 835−845. DOI：10.1016/j.rser.2013.12.020.

Riddick TM. 1944. The mechanism of corrosion of water pipes. Water Work Sand Sewerage, 133.

Ryznar JW, Langelier WF. 1944. A new index for determining amount of calcium carbonate scale formed by a water. Journal-American Water Works Association, 36(4): 472−486.

Song J, Liu M, Sun X. 2020. Model analysis and experimental study on scaling and corrosion tendencies of aerated geothermal water. Geothermics, 85: 101766. DOI：10.1016/j.geothermics.2019.101766.

Stahl G, Patzay G, Weiser L, et al. 2000. Study of calcite scaling and corrosion processes in geothermal systems. Geothermics, 29(1): 105−119. DOI：10.1016/S0375-6505(99)00052-8.

Tan XB, Wei SM, Bo BY, et al. 2019. Analysis of occurrence characteristics of geothermal resources and its relation to control structures in Zibo City, China. Journal of Groundwater Science and Engineering, 7(1): 70−76. DOI：10.19637/j.cnki.2305-7068.2019.01.007.

Wang GL, Lin WJ. 2020. Main hydro-geothermal systems and their genetic models in China. Acta Geologica Sinica, 94(7): 1923−1937. (in Chinese) DOI：10.19762/j.cnki.dizhixuebao.2020224.

Wang YX, Liu SL, Bian QY, et al. 2015. Scaling analysis of geothermal well from ganzi and countermeasures for anti-scale. Advances in New and Renewable Energy, 3: 202−206. DOI：10.3969/j.issn.2095-560X.2015.03.007.

Wei MH, Tian TS, Sun YD, et al. 2012. A study of the scaling trend of thermal groundwater in Kangding county of Sichuan. Hydrogeology Engineering Geology, 5: 132−138. (in Chinese) DOI：10.16030/j.cnki.issn.1000-3665.2012.05.029.

Yu Y, Zhou X, Fang B. 2007. Judgement and analysis of the scaling trend of thermal groundwater in Beijing's Urban Geothermal Fields. City Geology, 2(2): 14−18. (in Chinese)

Zarrouk SJ, Woodhurst BC, Morris C. 2014. Silica scaling in geothermal heat exchangers and its impact on pressure drop and performance: Wairakei binary plant, New Zealand. Geothermics, 51: 445−459. DOI：10.1016/j.geothermics.2014.03.005.

Zhang H, Hu YZ, Yun ZH, et al. 2016. Applying hydro-geochemistry simulating technology to study scaling of the high-temperature geothermal well in Kangding County. Advances in New and Renewable Energy, 4(2): 111−117. (in Chinese) DOI：10.3969/j.issn.2095-560X.

2016.02.006.

Zheng T, Stefánsson A, Kang FX, et al. 2023. Geochemical and isotope constraints on the hydrogeology and geochemistry of the geothermal waters in the Shandong Peninsula, China. Geothermics, 108: 102628. DOI：10.1016/j.geothermics.2022.102628.

Zhu JL, Yao T. 2004. Judgement and calculation of trend of corrosion and scaling of geothermal water. Industrial Water Use and Waste Water, 35(2): 23−25. (in Chinese)

Zhu JL. 2006. Geothermal energy development and application technology. The Chemical Industry Press. (in Chinese)